Inorganic Chemistry

ARTICLE

pubs.acs.org/IC

Extended Utility of Molten-Salt Chemistry: Unprecedented Synthesis of a Water-Soluble Salt-Inclusion Solid Comprised of High-Nuclearity Vanadium Oxide Clusters

Wendy L. Queen, J. Palmer West, Joan Hudson, and Shiou-Jyh Hwu*

Department of Chemistry, Clemson University, Clemson, South Carolina 29634-0973, United States

Supporting Information

ABSTRACT: Polyoxometallates (POMs) are desirable in materials applications ranging from uses as catalysts in selective oxidation reactions to molecular-like building blocks for the preparation of new extended solids. With the use of an unprecedented approach involving high temperature, molten salt methods, a fascinating series of salt-inclusion solids (SISs) that contain high nuclearity POMs has been isolated for the first time. $Cs_{11}Na_3(V_{15}O_{36})Cl_6$ (**1**) was synthesized using the eutectic NaCl/CsCl flux (mp 493 °C) which serves as a reactive solvent in crystal growth and allows for the SIS formation. Its framework can be viewed as an "ionic" lattice composed of alternately packed counterions of Cl-centered $[V_{15}O_{36}Cl]^{9-}$ clusters (V15; $S = 11/2$) and multinuclear $[Cs_9Na_3Cl_5]^{7+}$ cations. In light of the structural analysis, **1** was proven to be soluble in water giving rise to a dark green solution that is similar in color to single crystals of the title compound. Infrared spectroscopy of the solid formed from fast evaporation of the solution supports the presence of dissolved V15 clusters. Also noteworthy is the magnetization of **1** at 2 K, which reveals an s-shaped plot resembling that of superparamagnetic materials.

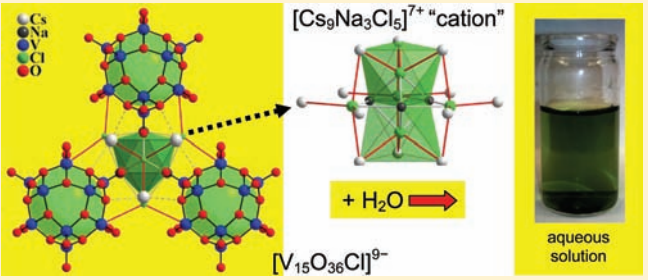

INTRODUCTION

Transition metal oxide (TMO) clusters, also known as polyoxometalates (POMs), offer an assortment of different structural motifs that serve as molecular-like building blocks for extended solids.[1] Prior to this investigation, POMs have been discovered using a variety of low-temperature methods such as hydrolytic aggregation in nonaqueous media,[2] conventional hydrothermal or solvothermal techniques,[3,4] and reductive aggregation processes.[5] Here we report the first POM containing material, $Cs_{11}Na_3(V_{15}O_{36})Cl_6$ (**1**), isolated using high-temperature, molten salt methods. It contains a Cl-centered $[V_{15}O_{36}Cl]^{9-}$ cluster and is the first report of a novel series of water-soluble, salt-inclusion solids (SISs). Similar cagelike polyoxovanadates (POVs) isolated thus far include $[V_{12}O_{32}]^{4-}$, $[V_{15}O_{36}]^{3,4,5-}$, $[V_{18}O_{42}]^{12-}$, $[V_{19}O_{49}]^{9-}$, and $[V_{34}O_{82}]^{10-}$ that reportedly encapsulate a wide variety of guest ions (X) such as Cl^-, Br^-, CO_3^{2-}, ClO_4^-, SCN^-, CH_3COO^-, and $HMoO_4^-$.[6−8] **1** contains the $[V_{15}O_{36}Cl]^{9-}$ cluster, which is the most reduced member of the $[V_{15}O_{36}X]^{n-}$ family (vide infra). The current discovery demonstrates the extended utility of molten salt chemistry in the exploratory synthesis of special framework solids that cannot otherwise be isolated by conventional methods.

POM aggregates, more frequently observed for early transition metals (such as V, Mo, and W), can vary in size, containing up to several hundred metal atoms fused together through oxygen ligation.[1] Although the history of these clusters can be traced back as early as 1826,[9] only within the last few decades have scientists really begun to reveal the rich structural chemistry and reactivity found within this distinct class of compounds.[10] The water-soluble, POM-containing SISs will enrich the exploration of new materials for already demonstrated applications that include, but are not limited to, supramolecular chemistry, catalysis, separations, and selective sorption.[11]

Recent reports of SISs have highlighted molten salt as a reactive solvent aiding in the synthesis of low-dimensional metal-oxide frameworks.[12] Although no reaction mechanism is known, one can imagine that the metal oxides are first "dissolved" in the "corrosive" molten salt and then, upon cooling, the covalent lattice begins to aggregate within and/or around the inherent structure of the molten ionic salt.[13] These all-inorganic SISs possess a fascinating structural chemistry where bonding at the interface of the dissimilar components appears to be directional. This template-like property has been revealed through the formation of porous frameworks,[14] noncentrosymmetric lattices,[15] and now for the first time, soluble magnetic TMO clusters.

In this paper, we report the synthesis and characterizations of the first water-soluble SIS, $Cs_{11}Na_3(V_{15}O_{36})Cl_6$ (**1**) synthesized in a reactive molten salt medium. The crystal structure analysis reveals that **1** is essentially a salt made of bulky counterions, $[V_{15}O_{36}Cl]^{9-}$ and $[Cs_9Na_3Cl_5]^{7+}$. Infrared spectroscopy of the solid from fast evaporation of the solution provides further

Received: July 26, 2011
Published: September 27, 2011

Table 1. Crystallographic Data for $Cs_{11}Na_3(V_{15}O_{36})Cl_6$ (1)

empirical formula	$Cs_{11}Na_3(V_{15}O_{36})Cl_6$
color/shape	dark green/cube
crystal size (mm^3)	0.10 × 0.05 × 0.02
formula weight (amu)	3083.78
space group, Z	*P*-6*m*2 (no. 187), 1
T, °C	25
a, Å	11.819(4)
c, Å	11.476(2)
V, $Å^3$	1388.3(7)
μ (Mo Kα), mm^{-1}	9.895
F_{000}	1373
d_{calcd}, g cm^{-3}	3.689
data/restraints/parameters	1005/0/80
secondary extinction	
reflections collected/unique	11873/1005
final R1/wR2[a] [$I > 2\sigma(I)$]	0.0359/0.1009
R1/wR2 (all data)	0.0374/0.1032
GOF	1.038
largest difference peak/hole ($e^-/Å^3$)	1.632/−1.212

[a] $R1 = \Sigma||F_o| - |F_c||/\Sigma|F_o|$; $wR2 = \{[\Sigma w(F_o^2 - F_c^2)^2]/[\Sigma w(F_o)^2)^2]\}^{1/2}$; $Rw = 1/[\sigma^2(F_o^2) + (0.0721P)^2 + 7.1276P]$, where $P = (F_o^2 + 2F_c^2)/3$

evidence for the dissolution of the title compound. Given the high nuclearity of the isolated $[V_{15}O_{36}Cl]^{9-}$ cluster, we also discuss the preliminary magnetization studies of **1**.

EXPERIMENTAL SECTION

All reactions were loaded in a nitrogen purged drybox, placed in silica ampules, and then flame-sealed under vacuum.

Synthesis. Single crystals of **1** were first discovered in a reaction that was designed to explore new manganese vanadate compounds. In the original reaction, MnO and V_2O_5 were mixed in a 1:1 mole ratio (~0.3 g) and added to a CsCl/NaCl eutectic flux equal to 3 times the mass of oxide reactants. The mixtures were heated to 650 °C, held there for 4 days, slowly cooled to 450 °C, and then furnace-cooled to room temperature. Green hexagonally shaped single crystals of **1** were retrieved in a yield <5%. There were also three other crystalline phases, with their approximate yield (%), $(CsCl)Mn_2(V_2O_7)$[15a] (≈ 10%), $Cs_{17}Cl_{15}Mn_{16.2}V_{1.8}O_6(Si_2O_5)_{18}$[16] (≈ 5%), and $NaMn_4(VO_4)_3$[16] (≈ 40%), in addition to an unidentified orange powder (≈ 20%). Despite the carbon coating, some silicon incorporation still resulted from the silica ampule.

After structure determination, a stoichiometric synthesis was carried out according to the determined chemical composition. Cs_3VO_4, V_2O_5, VO_2, NaCl, and CsCl were mixed in a 8:2:33:9:9 mole ratio (~0.75 g). The reactants were heated to 600 °C at a rate of 1 °C/min, isothermed for 4 days, and then furnace cooled to room temperature. A dark green polycrystalline powder was obtained. Single crystals, with dimensions smaller than 0.1 mm, can be grown using the same procedure with slow cooling (0.1 °C/min) to 400 °C followed by furnace cooling.

Infrared Spectroscopy. IR spectroscopy was carried out using a Magna IR spectrometer 550 (NICOLET) from a range of 4 000 to 400 cm^{-1}. Samples were prepared using approximately a 1:20 (by mass) mixture of **1** with spectral grade KBr. The mixture was ground and pressed into a pellet under 10 000 psi using a hydraulic press.

Magnetic Measurements. Magnetic susceptibility was measured with a Quantum Design SQUID MPMS-5S magnetometer. A ground polycrystalline samples (15.3 mg) was placed in a gel capsule. The initial temperature-dependent studies were performed over 2−300 K in applied fields of 100 Oe. The magnetic susceptibility was corrected for the contribution of the gel capsule and for the core diamagnetism (using Pascal Ms constants). Field-dependent measurements were performed with H up to ±50 000 Oe at 2−10 K.

Table 2. Bond Distances (Å) and Bond Angles (deg) for the $[V_{15}O_{36}Cl]$ Cluster in 1

V(1)O_5	O(4)−V(2)−O(4) 93.9(3)
V(1)−O(3) 1.61(1)	O(6)−V(2)−O(4) 104.8(2)
V(1)−O(2) 1.826(6)	O(4)−V(2)−O(4) 93.9(3)
V(1)−O(4) 1.896(6)	O(4)−V(2)−O(4) 78.5(3)
V(1)−O(4) 1.896(6)	O(4)−V(2)−O(4) 150.5(4)
V(1)−O(5) 1.99(1)	V(3)O_5
O(3)−V(1)−O(2) 102.1(6)	V(3)−O(1) 1.643(9)
O(3)−V(1)−O(4) 110.6(2)	V(3)−O(5) 1.919(3)
O(2)−V(1)−O(4) 91.1(2)	V(3)−O(5) 1.919(3)
O(3)−V(1)−O(4) 110.6(2)	V(3)−O(4) 1.940(6)
O(2)−V(1)−O(4) 91.1(2)	V(3)−O(4) 1.940(6)
O(4)−V(1)−O(4) 137.3(4)	O(1)−V(3)−O(5) 106.6(3)
O(3)−V(1)−O(5) 102.6(5)	O(1)−V(3)−O(5) 106.6(3)
O(2)−V(1)−O(5) 155.3(5)	O(5)−V(3)−O(5) 95.4(5)
O(4)−V(1)−O(5) 80.2(2)	O(1)−V(3)−O(4) 110.1(3)
O(4)−V(1)−O(5) 80.2(2)	O(5)−V(3)−O(4) 80.9(3)
V(2)O_5	O(5)−V(3)−O(4) 142.6(3)
V(2)−O(6) 1.62(1)	O(1)−V(3)−O(4) 110.1(3)
V(2)−O(4) 1.975(6)	O(5)−V(3)−O(4) 142.6(3)
V(2)−O(4) 1.975(6)	O(5)−V(3)−O(4) 80.9(3)
V(2)−O(4) 1.975(6)	O(4)−V(3)−O(4) 80.2(3)
V(2)−O(4) 1.975(6)	V(3)−V(1) 2.954(2)
O(6)−V(2)−O(4) 104.8(2)	V(3)−V(2) 3.006(2)
O(6)−V(2)−O(4) 104.8(2)	
O(4)−V(2)−O(4) 150.5(5)	V(1)−Cl(1) 3.523(2)
O(6)−V(2)−O(4) 104.8(2)	V(2)−Cl(1) 3.255(4)
O(4)−V(2)−O(4) 78.5(3)	V(3)−Cl(1) 3.458(2)

Crystallographic Studies. A dark green crystal, 0.15 mm × 0.09 mm × 0.03 mm, of **1** was selected under an optical microscope equipped with a polarizing light attachment. The data crystal was mounted on a glass fibers with epoxy for X-ray diffraction studies. The data was collected at room temperature on a four-circle Rigaku AFC8 diffractometer equipped with a Mercury CCD area detector, Mo Kα (λ = 0.710 73 Å) radiation. The structure was solved by the direct method using the SHELEX-97 program[17] and refined on F^2 by least-squares, full-matrix techniques; Table 1 reports the crystallographic data, and Table 2 reports selected bond distances and angles of **1**.

RESULTS AND DISCUSSION

Structure Description. **1** crystallizes in a hexagonal crystal system (*P*-6*m*2, no. 187). As shown in Figure 1 (top left), the extended structure consists of isolated $[V_{15}O_{36}Cl]^{9-}$ clusters spaced by multinuclear counterions made of Cs^+/Na^+ and Cl^- (vide infra). Compared to related derivatives, such as $[V_{15}O_{36}(PO_3)]^{8-}$, $[V_{15}O_{36}(CO_3)]^{7-}$, $[V_{15}O_{36}X]^{6-}$ (X = Cl^-, Br^-, or NO_3^-), $[V_{15}O_{36}Cl]^{5-}$, and $[V_{15}O_{36}Cl]^{4-}$, the cluster reported here is thus far the most reduced member of the $[V_{15}O_{36}X]^{n-}$ family discovered.[6,8] It is thought that heat, a natural source of reducing power, could induce the formation of the reduced $[V_{15}O_{36}Cl]^{9-}$ cluster. According to the structural formula derived from the single-crystal X-ray diffraction studies, the compound is mixed valent with formally 11 V^{4+} and 4 V^{5+} ions in each cluster.

dx.doi.org/10.1021/ic201605w |*Inorg. Chem.* 2011, 50, 11064–11068

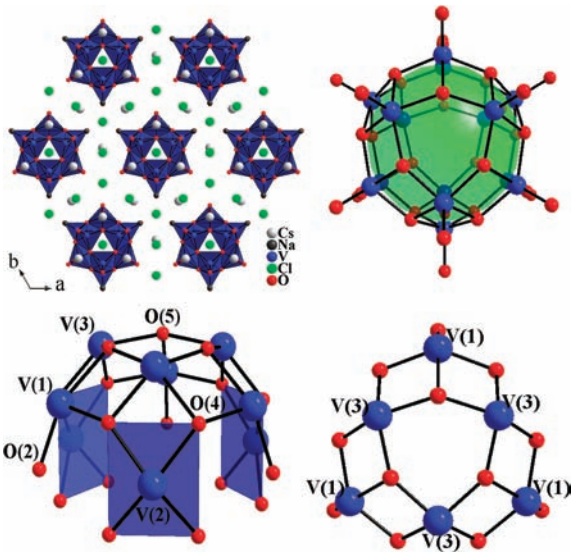

Figure 1. (top left) Projected view of a partial structure of **1**. (top right) Ball-and-stick representation of the $[V_{15}O_{36}Cl]^{9-}$ cluster. (bottom) Partial structures of the cluster showing the three crystallographically distinct vanadium sites. V(1) and V(3) form bowl-like caps located on the top and bottom of the D_{3h} $[V_{15}O_{36}Cl]^{9-}$ cluster. V(2) share oxygen atoms with three V(3), along with three V(1)−O(2)−V(1), to link the two bowls. All of the short V═O bonds are omitted for clarity.

Table 3. Bond Valence Sum Calculations[18] for 1

atom	V(1)	V(2)	V(3)
	1.588	1.566	1.464
	0.893	0.597 × 4	0.694 × 2
based on $r_o(V^{4+})$	0.739 × 2		0.656 × 2
	0.575		
	= 4.532	= 3.953	= 4.164
	1.671	1.649	1.541
	0.940	0.628 × 4	0.731 × 2
based on $r_o(V^{5+})$	0.778 × 2		0.691 × 2
	0.605		
	= 4.771	= 4.162	= 4.385

The charges of the vanadium cations are largely delocalized as suggested by the results of bond valence sum calculations,[18] Table 3. A successful stoichiometric-yield synthesis further confirms the chemical composition and oxidation states of the title compound (see the PXRD pattern in Figure S1 in the Supporting Information). Attempts to synthesize SISs containing previously reported lower valent vanadium oxide clusters, $[V_{15}O_{35}]^{3,4,5-}$, have not yet been successful.

In the $[V_{15}O_{36}Cl]^{9-}$ cluster, there are three crystallographically distinct vanadium sites. Like the less reduced $[V_{15}O_{36}]^{3,4,5-}$ clusters, each vanadium site adopts a VO_5 square pyramidal coordination with comparably short apical vanadyl (V═O) bonds, 1.61(1) Å, 1.62(2) Å, and 1.643(9) Å for V(1−3), respectively, pointing away from the center of the cage. The clusters, which exhibit D_{3h} point symmetry (Figure 1, top right), can be described as having two interlinked bowl-like caps in an eclipsed configuration. Each cap (Figure 1 bottom) consists of six VO_5 units made of alternating V(1)O_5 and V(3)O_5 polyhedra. The V(1)O_5 polyhedron shares two cis edges with neighboring

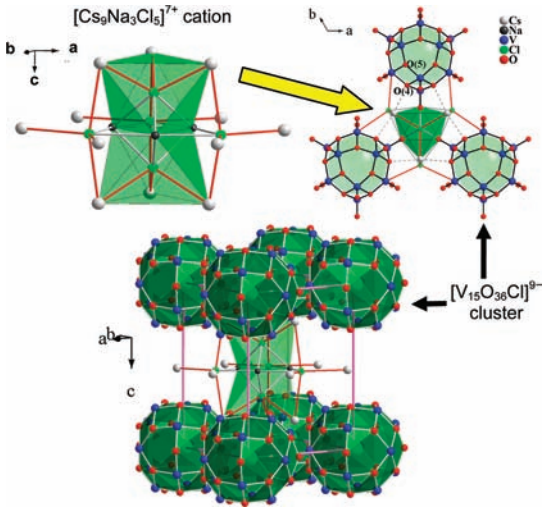

Figure 2. (top left) The $[Cs_9Na_3Cl_5]^{7+}$ multinuclear cation unit in **1**, see text for details. The thick lines are drawn to highlight the six-coordinate chlorine (d_{Cl-Na}, 2.773(3) Å × 3 and 2.987(6) Å × 2; d_{Cl-Cs}, 3.290(3) Å × 3, 3.476(4) Å × 2, and 3.576(9) Å × 2). (top right) Projected view showing the connectivity between the $[Cs_9Na_3Cl_5]^{7+}$ cation unit and three of six nearest $[V_{15}O_{36}Cl]^{9-}$ clusters. The other set of three clusters are in an eclipsed configuration relative to the set shown. Each cluster is connected to the cation unit by one Na−O bond (2.358(2) Å via one vanadyl oxygen atom (not shown because hidden behind the overlapped V═O bond) and two Cs−O (3.042(4) and 3.092(5) Å via a pair of the neighboring μ_3-O(4,5) atoms in the same cap), bonds shown as dotted gray lines. (bottom) The unit cell (outlined in solid purple lines) content showing the template effect of the multinuclear cation in the center, see text.

V(3)O_5 polyhedra, while V(3)O_5 shares trans edges with V(1)O_5 to close the cap. A pair of caps that form a bowl-like shape due to slightly distorted square pyramids is further linked by V(2) (Figure 1, bottom left) leading to a $[V_3(V_6O_{18})_2]$ alternative formulation of the cluster. The rest of the observed V−O bond distances, as listed in Table 2, range from 1.826(6) to 1.99(1) Å, which are comparable to 1.90−1.94 Å, the sum of the Shannon crystal radii for a six-coordinate $V^{4,5+}$ (including 5 V−O and 1 V−Cl) and O^{2-} (1.22 Å).[19]

The connectivity within the $[V_{15}O_{36}Cl]^{9-}$ cluster gives rise to 18 μ_3-oxo bridges (via 6 × O(4) and 3 × O(5) each cap) and three μ_2-oxo bridges (via O(2) found between the two eclipsed caps through V(1)−O(2)−V(1)), Figure 1, bottom left. The shortest metal−metal distances, 2.954(2) Å for V(1)−V(3) and 3.006(2) Å for V(2)−V(3), are found between edge-shared VO_5 units (Figure 1, bottom right). The cagelike cluster, found embedded in an ionic CsCl/NaCl matrix, encapsulates a Cl^- anion. The V−Cl distances, which are 3.523(2), 3.255(1), and 3.458(1) Å for V(1−3), respectively, are much longer than the expected sum of the Shannon crystal radii, 2.45−2.49 Å, for six-coordinate $V^{4,5+}$ and Cl (1.67 Å).[19] It was thought that the cage could possibly encapsulate larger ions; however, efforts made to synthesize other derivatives of **1**, including Br^- and I^-, have so far been unsuccessful with unidentifiable reaction products.

The structural analysis reveals that **1** is viewed as a salt composed of bulky counterions. Figure 2 shows the structure of the $[Cs_9Na_3Cl_5]^{7+}$ cation unit (top left) and its connectivity with three of six nearest $[V_{15}O_{36}Cl]^{9-}$ clusters (top right) that point toward the six Cs atoms on the top and bottom of the polyhedral core.

dx.doi.org/10.1021/ic201605w |*Inorg. Chem.* 2011, 50, 11064–11068

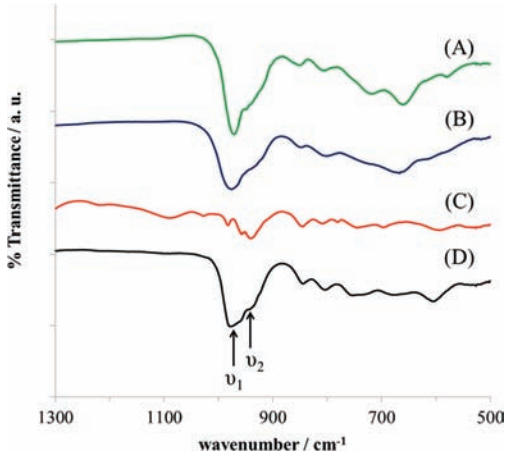

Figure 3. Selected IR bands (1300−500 cm^{-1} region) of (A) as-grown crystals **1**, (B) vacuum-dried green powder from freshly prepared solution of **1**, (C) selected orange crystals of $Cs_4Na_2V_{10}O_{28}\cdot 10H_2O$, and (D) mixed green and orange solids from a slightly aged solution, see text.

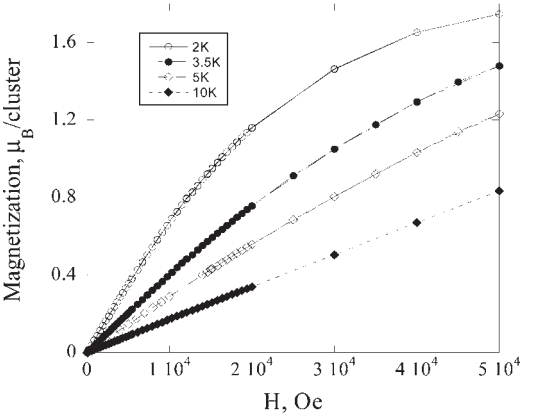

Figure 4. Field-dependent magnetization plot for **1** at various temperatures ranging from 2 to 10 K.

In each formula unit, the $[V_{15}O_{36}Cl]^{9-}$ anionic cluster is charge balanced by a multinuclear $[Cs_9Na_3Cl_5]^{7+}$ cation in addition to 2 mol of Cs^+. The former cation, as shown in Figure 2 (top left), is made of two fused, Cl-centered antitrigonal prisms ($Cl@Na_3Cs_3$, in polyhedral drawing) and three octahedra ($Cl@Na_2Cs_4$, in ball-and-stick representation). As anticipated, Cl adopts six-coordination like that in NaCl. The coordination of Na^+ and Cs^+ ions, however, appears to be less complete by additional coordination with oxide anions of the covalent cluster, $[V_{15}O_{36}Cl]^{9-}$. This leads to the electrostatic interaction between the counterions and thus the ionic character of the whole lattice. Nevertheless, this multinuclear cation is elegantly stabilized by $[V_{15}O_{36}Cl]^{9-}$, as shown in Figure 2 (bottom) and Figure S2 in the Supporting Information, where the structure drawings help possibly discern the packing of size matchable "counter ions", which arguably implies a thermodynamic origin of the lattice.

It is evident that **1** is soluble in water giving rise to a dark green solution that is similar in color to single crystals of the title compound. When the solution stands over a period of 2 days at room temperature, however, it starts turning an orange/yellow tint. Dark yellow single crystals begin to fall out after sitting in the sunlight in a capped vial for ∼2 weeks. The crystals from the aged solution were identified by single-crystal X-ray diffraction to be a known phase, $Cs_4Na_2V_{10}O_{28}\cdot 10H_2O$, that contains fully oxidized $[V_{10}O_{28}]^{6-}$ anions.[20] From this observation, we speculate that the reduced $[V_{15}O_{36}Cl]^{9-}$ anion is subject to oxidative decomposition in aqueous media.

IR Studies. Infrared (IR) studies provide further evidence for the presence of the $[V_{15}O_{36}Cl]^{n-}$ cluster in aqueous solution. Figure 3 reveals that the IR spectra (1300−500 cm^{-1}) obtained from as-grown green crystals of **1** (spectrum A) and a green powder acquired from a fast evaporation of a solution containing **1** (spectrum B) possess all of the same distinctive vibrational bands at ∼984 cm^{-1} (υ_1) and/or 949 cm^{-1} (υ_2) corresponding to V═O stretching modes. Further, we have obtained an IR spectra of selected yellow crystals of only the decomposition product, $Cs_4Na_2V_{10}O_{28}\cdot 10H_2O$ (spectrum C), which is comparable with that reported in ref 20) and a mixture of the green and yellow crystals obtained from a slightly aged solution of **1** (spectrum D). While spectra A and B look the same, due only to the presence of V15 clusters, spectrum D appears to be a combination of the spectra A and C suggesting an incomplete decomposition of the most reduced $[V_{15}O_{36}Cl]^{9-}$ in the slightly aged solution. It is worth noting that attempts were made to capture a $[V_{15}O_{36}Cl]$ cluster using high-resolution transmission electron microscopy (HRTEM) but were unsuccessful possibly due to the thermal instability of the reduced cluster under the electron beam; however, ongoing investigations for the direct evidence of the cluster and its oxidation state (n) via controlled dissolution processes are underway.

Magnetic Studies. In light of the high nuclearity cluster contained in **1** ($S = 11/2$ per V15 cluster), preliminary magnetic measurements were performed on a powder sample obtained from the stoichiometric-yield synthesis. The molar magnetic susceptibility (χ) and the inverse molar magnetic susceptibility (χ^{-1}) of **1** are plotted in Figure S3 in the Supporting Information. The effective magnetic moment, $\mu_{eff} = 2.83(\chi_M T)^{1/2}$, was plotted as a function of temperature, Figure S3 (inset) in the Supporting Information. It gradually decreases from 5.41 μ_B at 300 K to 3.65 μ_B at 50 K and then becomes nonlinear with a more pronounced decrease below 25 K to 2.57 μ_B at 2 K. These values are smaller than the anticipated magnetic moment, 5.74 μ_B, for 11 V^{4+} cations ($S = {}^1/_2$), possibly indicating intracluster antiferromagnetic (AFM) exchange, similarly observed in other reduced POVs.[6a] From these plots, there is no evidence of the development of long-range magnetic order. However, on the basis of the close proximity of μ_3-oxo-bridged metal centers within the clusters, creating multiple geometrically frustrated exchange pathways, a nonzero AFM (or FM) exchange is expected.

Isothermal magnetization data was obtained from **1** in fields ranging from ±50 000 Oe and temperatures from 2 to 10 K (Figure 4). The field-dependent plot shows a decrease in the magnitude of the magnetization plot as a function of increasing temperature. At 2 K, the magnetization plot has an s-shape, similarly observed for superparamagnetic materials, which reaches an unsaturated maximum of approximately 1.6 μ_B/cluster at a maximum applied field of 50 000 Oe. Although not trivial due to a large number of competing magnetic exchange pathways, **1** shows no long-range magnetic ordering, as mentioned above, and an s-shape hysteresis, which are reportedly indicative of molecular-like magnetic behavior. Detailed magnetic analysis is awaiting further studies including ESR and inelastic neutron scattering[21] that will probe the ground-state spin structure of this mixed-valent POV cluster.

dx.doi.org/10.1021/ic201605w |*Inorg. Chem.* 2011, 50, 11064–11068

Final Remarks. Our current study seems to suggest that high-temperature methods enable the formation of further reduced vanadium oxide clusters that cannot otherwise be isolated via low-temperature reactions. The observation of the $[Cs_9Na_3Cl_5]^{7+}$ cation is also intriguing as the Cl^- ions adopt the same local coordination as that in the NaCl lattice. We anticipate the isolation of more multinuclear cations, which can provide empirical evidence relevant to theoretical studies of the inherent structure of a molten salt, as cited in ref 13. In this study, nonmagnetic, multinuclear cations, like organic templates in molecular magnets, space and structurally confine the V15 magnetic clusters. From a synthetic standpoint, this work also opens up new opportunities in our current pursuit of new quantum magnetic solids within extended systems.[22,23] Other studies of **1** include electrochemical investigations of the highly reduced $[V_{15}O_{36}Cl]^{9-}$ cluster in aqueous solution. It would be interesting to perform multielectron oxidation of the $[V_{15}O_{36}X]^{n-}$ family for those clusters already isolated in solids (for n = 9, 6, 5, 4) and investigate the possible existence of intermediate oxidation states (n = 8, 7, <4) that are yet to be discovered. Nevertheless, the current discovery has already enticed further exploration of POM-containing, water-soluble SISs in molten-salt media,[16] and their results will be published shortly.

■ ASSOCIATED CONTENT

Supporting Information. X-ray crystallographic file (in CIF format), PXRD patterns, structure drawings of the packing of counterions, and molar magnetic susceptibility plots. This material is available free of charge via the Internet at http://pubs.acs.org.

■ AUTHOR INFORMATION

Corresponding Author
*E-mail: shwu@clemson.edu.

■ ACKNOWLEDGMENT

This work has been supported by the National Science Foundation (NSF, Grant DMR-0706426). The support for the purchase of a SQUID magnetometer (Grant CHE-9808044) and an X-ray diffractometer (Grants ESR-9108772, CHE-9207230, and 9808165) from the NSF are also gratefully acknowledged.

■ REFERENCES

(1) Pope, M. T.; Müller, A. Introduction to Polyoxometalate Chemistry: From Topology via Self- Assembly to Applications. In *Polyoxometalate Chemistry: From Topology via Self-Assembly to Applications*; Pope, M. T., Müller, A., Eds.; Kluwer: New York, 2001; pp 1−6.

(2) Errington, R. J. Rational Approaches to Polyoxometalate Synthesis. In *Polyoxometalate Chemistry: From Topology via Self-Assembly to Applications*; Pope, M. T., Müller, A., Eds.; Kluwer: New York, 2001; pp 7−22.

(3) Salta, J.; Chen, Q.; Chang, Y.-D.; Zubieta, J. *Angew. Chem., Int. Ed. Engl.* **1994**, *33*, 757–760.

(4) (a) Khan, M. I.; Zubieta, J. *Prog. Inorg. Chem.* **1995**, *43*, 1–149. (b) Chang, Y.-D.; Salta, J.; Zubieta, J. *Angew. Chem., Int. Ed. Engl.* **1994**, *33*, 325–327. (c) Chen, Q.; Zubieta, J. *Angew. Chem., Int. Ed. Engl.* **1993**, *32*, 261–263.

(5) (a) Müller, A.; Polarz, S.; Das, S. K.; Krickmeyer, E.; Bögge, H.; Schmidtmann, M.; Hauptfleisch, B. *Angew. Chem., Int. Ed* **1999**, *38*, 3241–3245. (b) Müller, A.; Krickmeyer, E.; Bögge, H.; Schmidtmann, M.; Peters, F. *Angew. Chem., Int. Ed.* **1998**, *37*, 3360–3363. (c) Maestre, J. M.; Poblet, J. M.; Bo, C.; Casañ-Pastor, N.; Gomez-Romero, P. *Inorg. Chem.* **1998**, *37*, 3444–3446.

(6) (a) Dong, B.; Gómez-García, C. J.; Peng, J.; Benmansour, S.; Ma, J. *Polyhedron* **2007**, *26*, 1310–1316. (b) Müller, A.; Penk, M.; Rolfng, R.; Krickemeyer, E.; Döring, J. *Angew. Chem., Int. Ed. Engl.* **1990**, *29*, 926–927.

(7) (a) Suber, L.; Bonamico, M.; Fares, V. *Inorg. Chem.* **1997**, *36*, 2030–2033. (b) Müller, A.; Sessoli, R.; Krickemeyer, E.; Bögge, H.; Meyer, J.; Gatteschi, D.; Pardi, L.; Westphal, J.; Hovemeier, K.; Rolfing, R.; Doring, J.; Hellweg, F.; Beugholt, C.; Schmidtmann, M. *Inorg. Chem.* **1997**, *36*, 5239–5250. (c) Müller, A.; Rolfng, R.; Döring, J.; Penk, J. M. *Angew. Chem., Int. Ed.* **1991**, *30*, 588–590. (d) Day, V. W.; Klemper, W. G.; Yaghi, O. M. *J. Am. Chem. Soc.* **1989**, *111*, 5959–5961. (e) Müller, A.; Penk, M.; Krickemeyer, E.; Bögge, H.; Wallberg, H.-J. *Angew. Chem., Int. Ed. Engl.* **1988**, *27*, 1719–1721. (f) Müller, A.; Krickemeyer, E.; Penk, M.; Wallberg, H.-J.; Bögge, H. *Angew. Chem., Int. Ed. Engl.* **1987**, *26*, 1045–1046. (g) Johnson, G. K.; Schlemper, E. O. *J. Am. Chem. Soc.* **1978**, *100*, 3645–3646.

(8) (a) Hayashi, Y.; Miyakoshi, N.; Shinguchi, T.; Uehara, A. *Chem. Lett.* **2001**, 170–171. (b) Drezen, T.; Ganne, M. *J. Solid State Chem.* **1999**, *147*, 552–560. (c) Yamase, T.; Ohtaka, K. J. *Chem. Soc., Dalton Trans.* **1994**, 2599–2608. (d) Müller, A.; Rohlfing, R.; Krickemeyer, E.; Bögge, H. *Angew. Chem., Int. Ed. Engl.* **1993**, *32*, 909–912.

(9) Bielański, A.; Lubańska, A.; Micek-Ilnicka, A.; Poźniczek, J. *Coord. Chem. Rev.* **2005**, *249*, 2222–2231.

(10) Khan, M. I. *J. Solid State Chem.* **2000**, *152*, 105–112.

(11) (a) Sloboda-Rozner, D.; Witte, P.; Alsters, P. L.; Neumann, R. *Adv. Synth. Catal.* **2004**, *346*, 339–345. (b) Hagrman, P. J.; Hagrman, D.; Zubieta, J. *Angew. Chem., Int. Ed.* **1999**, *38*, 2638–2684. (c) Braun, P. V.; Osenar, P.; Tohver, V.; Kennedy, S. B.; Stupp, S. I. *J. Am. Chem. Soc.* **1999**, *121*, 7302–7309. (d) Müller, A.; Peters, F.; Pope, M. T.; Gatteschi, D. *Chem. Rev.* **1998**, *98*, 239–271. (e) Müller, A.; Reuter, H.; Dillinger, S. *Angew. Chem., Int. Ed.* **1995**, *34*, 2328–2861. (f) Huan, G.; Greaney, M. A.; Jacobson, A. J. *J. Chem. Soc. Chem. Commun.* **1991**, *4*, 260–261.

(12) (a) Hwu, S.-J.; Ulutagay-Kartin, M.; Clayhold, J. A.; Mackay, R.; Wardojo, T. A.; O'Connor, C. T.; Krawiec, M. *J. Am. Chem. Soc.* **2002**, *124*, 12404–12405. (b) Huang, Q.; Kartin, M.; Mo, X.; Hwu, S.-J. *Mater. Res. Soc. Symp. Proc.* **2002**, 459–464. (c) Ulutagay, M.; Schimek, G. L.; Hwu, S.-J.; Taye, H. *Inorg. Chem.* **1998**, *37*, 1507–12.

(13) La Violette, R. A.; Budzien, J. L.; Stillinger, F. H. *J. Chem. Phys.* **2000**, *112*, 8072–8078.

(14) (a) Huang, Q.; Hwu, S.-J.; Mo, X. *Angew. Chem., Int. Ed.* **2001**, *40*, 1690–1693. (b) Huang, Q.; Ulutagay, M.; Michener, P. A.; Hwu, S.-J. *J. Am. Chem. Soc.* **1999**, *121*, 10323–10326.

(15) (a) Queen, W. L.; West, J. P.; Hwu, S.-J.; VanDerveer, D. G.; Zarzyczny, M. C.; Pavlick, R. A. *Angew. Chem., Int. Ed.* **2008**, *47*, 3791–3794. (b) Mo, X.; Ferguson, E.; Hwu, S.-J. *Inorg. Chem.* **2005**, *44*, 3121–3126. (c) Mo, X.; Hwu, S.-J. *Inorg. Chem.* **2003**, *42*, 3978–3980. (d) Huang, Q.; Hwu, S.-J. *Inorg. Chem.* **2003**, *42*, 655–657. (e) Etheredge, K. M. S.; Hwu, S.-J. *Inorg. Chem.* **1995**, *34*, 3123–3125.

(16) Queen, W. L. Ph.D. Dissertation, Clemson University, Clemson, SC, 2008.

(17) (a) Sheldrick, G. M. In *Crystallographic Computing 3*; Sheldrick, G. M., Kruger, C., Goddard, R., Eds.; Oxford University Press: London, 1985; pp 175−189. (b) Sheldrick, G. M. *SHELXTL*, version 6.1; Structure Determination Software Programs; Bruker Analytical X-ray Systems Inc.: Madison, WI, 2001.

(18) (a) *VALENCE* for DOS, version 2.0: Brown, I. D. *J. Appl. Crystallogr.* **1996**, *29*, 479−480. (b) Brown, I. D.; Altermatt, D. *Acta Crystallogr.* **1985**, *B41*, 244–247.

(19) Shannon, R. D. *Acta Crystallogr.* **1976**, *A32*, 751–767.

(20) Piro, O. E.; Varetti, E. L.; Brandán, S. A.; Altabef, A. B. *J. Chem. Crystallogr.* **2003**, *33* (1), 57–63.

(21) Basler, R.; Chaboussant, G.; Sieber, A.; Andres, H.; Murrie, M.; Kögerler, P.; Bögge, H.; Crans, D. C.; Krichemeyer, E.; Janssen, S.; Mutka, H.; Müller, A.; Güdel, H.-U. *Inorg. Chem.* **2002**, *41*, 5675–5685.

(22) Hwu, S.-J. *Chem. Mater.* **1998**, *10*, 2846–2859.

(23) (a) West, J. P.; Queen, W. L.; Hwu, S.-J.; Michaux, K. E. *Angew. Chem., Int. Ed.* **2011**, *50*, 3780–3783. (b) Queen, W. L.; Hwu, S.-J.; Wang, L. *Angew. Chem., Int. Ed.* **2007**, *46*, 5344–5347.